

This work has been submitted to **NECTAR**, the **Northampton Electronic Collection of Theses and Research**.

Article

Title: 'Local gradient' and between-site variability of erosion rate on badlands in the Karoo, South Africa

Creators: Favis-Mortlock, D., Boardman, J., Foster, I. D. L. and Greenwood, P.

DOI: [10.1002/esp.4293](https://doi.org/10.1002/esp.4293)

Example citation: Favis-Mortlock, D., Boardman, J., Foster, I. D. L. and Greenwood, P. (2017) 'Local gradient' and between-site variability of erosion rate on badlands in the Karoo, South Africa. *Earth Surface Processes and Landforms*. 0197-9337. (In Press)

It is advisable to refer to the [publisher's version](#) if you intend to cite from this work.

Version: Accepted version

Official URL: <http://dx.doi.org/10.1002/esp.4293>

Note: This is the peer reviewed version of the article, which has been published in final form at <http://dx.doi.org/10.1002/esp.4293>. This article may be used for non-commercial purposes in accordance with Wiley Terms and Conditions for Self-Archiving.

<http://nectar.northampton.ac.uk/10030/>



‘Local gradient’ and between-site variability of erosion rate on badlands in the Karoo, South Africa

David Favis-Mortlock^{1*}, John Boardman¹, Ian Foster^{2,3}, and Philip Greenwood⁴

¹*Environmental Change Institute, Oxford University Centre for the Environment, Oxford, UK*

²*Faculty of Arts, Science and Technology, University of Northampton, Northampton, UK*

³*Department of Geography, Rhodes University, Grahamstown, Eastern Cape, South Africa*

⁴*Physical Geography and Environmental Change, Department of Environmental Sciences, University of Basel, Klingelbergstrasse 27, Basel 4056, Switzerland*

*Correspondence to: D. Favis-Mortlock, Environmental Change Institute, Oxford University Centre for the Environment, South Parks Road, Oxford OX1 3QY, UK. Email: david.favis-mortlock@ouce.ox.ac.uk

Abstract

Site-average values of local gradient, defined as the steepest slope angle measured at a point, are a powerful predictor of long-term rates of soil loss as measured by erosion pins on the non-channel floor portions of ten badland study sites in the Karoo area of South Africa. Local gradient may be easily measured using a smartphone clinometer. The successful use of local gradient here is in strong contrast to the previous failure of other site-specific attributes, including other measures of gradient and relief, to explain between-site variation in erosion rate on these study sites.

Each measurement of local gradient may be thought of as a sample of the site’s microtopography. Microrelief is a strong determinant of the emergent patterns of inter-channel overland flow, and hence of the patterns of inter-channel erosion by flow. Local gradient changes most rapidly during the initial stages of channel incision. When channels are established, local gradient changes more slowly leading to almost-parallel retreat of channel sidewalls.

A sensitivity analysis suggests that measurements of local gradient are not all equal with regard to prediction of long-term erosion rate. A greater share of predictive power is contributed by measurements made on very steep or vertical channel side wall areas, and a lesser share is contributed by measurements made on interfluves.

Keywords:

Soil erosion, local gradient, clinometer app, microtopography, badlands, Karoo

1. Introduction

1.1 The study sites

The environmental history of the Sneeuberg uplands in the eastern Karoo, South Africa, has been the subject of almost 20 years of research by an international group (Boardman et al., 2017). One focus of the work has been erosion rates on badlands. Annual monitoring of 10 badland study sites began in 2001 (Keay-Bright and Boardman, 2009). This monitoring has continued to the present; the current paper updates results to November 2016 (Table 1).

*** TABLE 1

*** FIGURE 1

These study sites (Figure 1) are remote: access is difficult and the area sparsely populated. Elevations in the study area are between 1698 and 1755 m, with high ground comprised of Triassic Katberg Formation sandstone and mudstone with dolerite intrusions. Lower ground is underlain by Permian Balfour Formation shales and sandstones, with up to 6 m of Quaternary colluvium and alluvium overlying bedrock on footslopes and valley bottoms (Holmes et al., 2003; Boardman et al., 2005). The badlands considered here are incised into this colluvium. The Klein Seekoi (Small Seacow) river drains the area; this is a north-flowing headwater tributary of the Orange.

Full descriptions of the badland study sites and the methods of measurement are given in Boardman et al. (2015). In summary: the sites are not identical, since they were selected to represent a reasonable sample of the badland component of the landscape. All include small areas of the original surface of the colluvium. This remains as interfluvies, on which the soil is highly compacted (Boardman et al., 2003). These interfluvies separate channels of various sizes, from rill-sized up to (on two sites) gully-sized. Channel networks may be complex, however there is a tendency for channels to be oriented approximately down the hillslope (i.e. down the slope of the original colluvial surface).

At each site, 25 erosion pins were installed in a 5 pin x 5 pin grid. Pin spacing is 1 x 1 m at six sites and 1 m x 2 m at four sites, at which the longer edge of the pin grid is oriented approximately down the hillslope. Changes in pin exposure were measured at roughly annual (and sometimes shorter) intervals. These measurements permit estimates to be made of long-term erosion and accumulation rates (Boardman et al., 2015; Boardman and Favis-Mortlock, 2016). Note that the study sites are, in effect, unbounded plots.

1.2 Rainfall data

No official meteorological station raingauges operate close to the study sites. The nearest official meteorological station is c. 55 km to the north-east, at Grootfontein agricultural research station near Middelburg. Collection of daily rainfall data began at Grootfontein in 1878. Sub-daily rainfall data were collected only for a very short period: collection has now been abandoned.

Therefore in this and in earlier studies we make use of informal daily rainfall data gathered by local farmers. No sub-daily rainfall data are collected. We judge this daily data to be generally reliable: see Boardman et al. (2015). The daily rainfall data used here are from a farmer-operated raingauge which was situated at Compassberg Farm (within 5 km of all erosion pin sites: Figure 1) from 1987 until January 2010, when it was moved to Lucernvale Farm (within 7 km of all erosion pin sites: Figure 1). In February 2016 the raingauge was moved back to Compassberg Farm. We assume that this combined Compassberg-Lucernvale-Compassberg rainfall record applies to all ten study sites.

The temporal pattern of rainfall measured by this gauge is strongly seasonal, with most precipitation falling between January and March (Foster et al., 2007). The number of rain-days per year is low (an average of 36 between 2000 and 2015, with a maximum of 56 and a minimum of 26).

1.3 Runoff and erosion processes on the study sites

The remoteness of the sites poses problems regarding rainfall data. It creates further difficulties with regard to the collection of runoff and erosion data. Practical considerations mean that site visits are only possible at approximately annual intervals. Thus monitoring of runoff using (for example) troughs is infeasible. Again, farmer observations can be useful; but quantitative observations of runoff are only possible if a site visit happens to coincide with a rainfall event. On such occasions, we have observed shallow runoff (a few cm deep) in the channels after only 10 mm rainfall (Figure 2). Flow on the inter-channel areas is never more than a few mm in depth.

***** FIGURE 2**

Infrequent access also constrains observation of the processes which give rise to erosion and accumulation on the study sites. We assume that weathering is largely driven by wetting and drying (Boardman et al., 2017). Splash redeposition of weathered material certainly occurs: splashed material is often found stuck to the erosion pins. However, the relative importance of splash and runoff in terms of moving weathered sediment on these sites is unknown.

Nonetheless, some inferences are possible. Splash redistribution is more effective on steep slopes (De Ploey and Savat, 1968) such as the channel side slopes of our study sites, whilst runoff is probably the dominant process on the relatively flat and compacted interfluvies. In addition, since weathered material is removed by flow, we can infer there will be sediment available for splash redistribution only if there has been a sufficiently long period of weathering following the last rainfall event. We can further deduce that runoff will be relatively sediment-free if two rainfall events occur in close temporal proximity, since little weathered material will have accumulated prior to the second rainfall event. A longer interval between rainfall events implies more sediment-rich runoff.

1.4 Between-site variability in erosion rate

Previous work (Boardman et al., 2015) shows that erosion rates on the ten sites, as measured by the erosion pins, are sufficiently similar for them to be considered to be drawn from the same statistical population. Thus from one statistical perspective, these ten sites are replicates. Nevertheless, there are obvious inter-site differences in erosion rate, which are greater than the errors associated with pin measurement (see Table 3 in Boardman et al., 2015). But between-site variation in erosion, accumulation and net erosion (i.e. erosion minus accumulation) does not follow any clear pattern. Despite much experimentation, none of the site characteristics shown in Table 2 have been able to explain between-site variation in erosion, accumulation or net erosion.

***** TABLE 2**

That none of these attributes – not even those related to slope or relief – can shed light on inter-site variation is surprising. It has been a geomorphological truism since at least Gilbert (1877, p96) that gradient (we use this more precise but less common word in preference to the more common but rather ambiguous term ‘slope’) is a major control on erosion by rain and flowing water. On conventional erosion plots, the ‘overall gradient’ (i.e.

the difference in elevation between the highest and lowest points) has long been used as an effective predictor of erosion rate (e.g. Wischmeier and Smith, 1978).

1.5 Within-site relief and measures of gradient

Defining a representative gradient for each of our study sites is not straightforward. We considered several possible approaches.

Any measure of gradient comprises a difference in elevation paired with some horizontal length. The simplest approach to representing the gradient at each site is to use a single elevation-length pair per site; and an obvious way of doing this is to subtract the elevations of the highest and lowest points on each site, and to choose a horizontal length such as that of the pin grid. However, the complex within-site relief (Table 2: see also Figure 2 in Boardman et al., 2015) renders this simple 'overall gradient' approach close to meaningless, as well as potentially unrepresentative: on the C1 (see Table 1 for site abbreviations) site for example, there is a near-vertical gradient underlying a small part of the pin grid, with gentle gradients elsewhere.

An alternative single-gradient approach is to use the 'hillslope gradient'. We define this as the maximum gradient of the remnant of the slope that pre-dates channel incision and badland development. However, objectively capturing the hillslope gradient is not easy, again because of current within-site relief. We found hillslope gradient to be an ineffective predictor of current erosion rates on each site (Table 2).

We therefore abandoned the notion of employing a single measurement of gradient to characterise each site, and instead chose to use multiple measurements per site. An obvious approach would be to construct a Digital Elevation Model (DEM) for each site using e.g. laser scanning or photogrammetry, and to then extract gradients at sample points. However, the remoteness of the study sites has, so far, made the transport and use of the necessary equipment impractical.

We therefore considered other simple approaches to capturing gradient at multiple within-site locations, and eventually decided to measure 'local gradient'. We define local gradient as the steepest slope angle, measured over a fixed length (here 13 cm), immediately adjacent to each erosion pin. This paper thus focuses on our attempts to relate local gradient to pin-measured erosion rates at each of our study sites.

1.6 Topographic category

Given the strong relief that has developed on each site, it seemed reasonable to assume that local gradient would not be an equally important determinant of erosion everywhere on the site. Thus we made use of the notion of pins representing different within-site 'topographic categories' (Boardman et al., 2017). When pin exposure was recorded, we assigned the erosion pin to one of the following five topographic categories:

- a: broad flat interfluvium
- b: very steep or vertical channel side wall
- c: channel floor
- d: footslope
- e: narrow interfluvium between channels.

Examples of the five topographic categories are shown in Figure 3. Assigning these does of course involve an element of subjective judgement, e.g. regarding the width of the interfluvium when distinguishing categories a and e. Consistency in identifying topographic

category is therefore vital. Also, note that the topographic category assigned to a pin may change over time.

*** FIGURE 3

2. Method

In November 2016, an Android cellphone app was used to measure maximum gradient in degrees immediately adjacent to each of the 25 erosion pins at the 10 pin sites.

*** FIGURE 4

The app is called Clinometer. The authors claim it to be the most precise slope measurement tool for Android devices; digital readings are given to 0.1 degrees. It is produced by Plaincode Tools™ and can be freely downloaded from the Android App Store (Figure 4). Measurements of local gradient were obtained by holding a mobile phone (Motorola Moto-G) with the centre of its long axis against the pin and along the ground, and with the next-longest axis of the phone held vertically. Readings were taken after the digital screen had settled to a constant value for 3-5 seconds.

The phone was rotated around the base of each pin, touching the pin, to obtain the maximum downslope angle. Each measurement took between 30 and 90 seconds, however this was slower where maximum gradient was not immediately obvious. By conducting repeat tests, we estimate that the error in these measurements of local gradient is small, and certainly less than 1 degree.

Results were analysed using a Python script which was run using Python 3.5.2 with the following libraries: NumPy 1.11.1 and SciPy 0.17.1. All graphs were produced using Matplotlib 1.5.2.

3. Results

3.1 Local gradient and topographic category

*** TABLE 3

Table 3 shows percentages of pin measurements assigned to each topographic category, plus long-term rates of erosion, accumulation and net erosion for each topographic category. There are no obvious patterns. Pins in topographic category d are the most common. Pins in topographic category e are the least common: there are no pins in this category at four sites. Erosion rates (expressed as an average for all ten sites) are highest for category d. However this is not true for all sites: for three sites category a has the highest erosion rate, whilst at site C2 category c has the highest erosion rate. Accumulation (average for all ten sites) is highest for category c. Net erosion (average for all ten sites) is highest for category a, with the value for category d only slightly smaller. Note that at three sites, category c showed negative net erosion i.e. net accumulation; however these are not the sites at which along-channel downcutting has reached bedrock.

Of these 250 local gradient measurements, 61 measurements were omitted from subsequent analysis because the topographic category for the associated erosion pin had changed since the start of measurements. Figure 5 shows the distributions of the remaining 189 local gradient measurements, by site.

*** FIGURE 5

Distributions of local gradient are positively skewed for all sites. On one site (C1), measurements range from near horizontal to near vertical. Figure 6 shows the local gradient measurements split by topographic category. Distributions are positively skewed for all topographic categories, with the greatest skewness for topographic category b (very steep or vertical channel side wall). The lowest average value of local gradient is for topographic category c (channel floor).

*** FIGURE 6

For all 31 possible combinations of the five topographic categories, ten values of site-average local gradient (in degrees and converted to per cent slope) were calculated, and each value regressed against that site's average erosion, accumulation, and net erosion rates. For each combination of topographic categories, if the topographic category assigned to a pin resulted in that pin being excluded, then all data from that pin (local gradient, erosion, accumulation, and net erosion) were omitted. Thus all 189 local gradient measurements were used only for those analyses which included pins of all topographic categories (i.e. categories a, b, c, d, and e). While data from all ten sites could be used for most combinations, a few combinations of topographic category (e.g. category e only) resulted in sites with no pins with this combination of category. Such sites were then omitted from the analysis of this combination of topographic categories.

3.2 Local gradient and erosion

Table 4 summarizes the results of the regressions for site-average erosion.

*** TABLE 4

The best fit ($r^2 = 0.918$, significant at 99.99%, N sites = 10, N pins = 158: see the top row of Table 4) was obtained with site-average local gradient expressed as per cent slope, for topographic categories a, b, d, and e (i.e. with topographic category c omitted). Figure 7 shows this regression, along with the number of pins included from each site. Note that the values of erosion rate for each site here are not identical to those shown in Table 1, since some pins have been omitted.

*** FIGURE 7

Further regressions were carried out using more sophisticated transformations of the site-average local gradient: the USLE S-factor as revised by Liu et al. (1994) and by Nearing (1997). These variants of the USLE S-factor were selected because of their suggested suitability for gradients exceeding 20-30 per cent. However, results using these USLE-based expressions of local gradient differed little from the initial results. As with the initial results, regressions using topographic categories a, b, d and e (as in Figure 7) consistently gave the best fit for the USLE-based regressions.

A third series of regressions was carried out using site-median, rather than site-average, local gradient: this seemed a potentially useful alternative, given the skewness of the distributions of local gradient (Figures 5 and 6). Site-median local gradient was regressed against site-average erosion, accumulation, and net erosion for all combinations of topographic category, with site-median local gradient again expressed as degrees, as per cent, and as Liu et al. (1994) and Nearing (1997) S-factor variant. Results were again broadly similar to the first set of regressions, but with generally lower r^2 and significance. Using site-median local gradient, the best fit was consistently obtained with topographic categories a, b, c and d.

A final series of regressions focused on erosion rate vs local gradient as measured for individual pins (rather than site-average local gradient). This could be done meaningfully only with the pins for all sites combined, since some sites had no, or very few pins, for several of the topographic categories. For this final series of regressions the best fit ($r^2 = 0.237$, significant at 99%) was very poor compared with earlier results; this was for per-pin local slope in percent, and for topographic category d only (Figure 8).

*** FIGURE 8

3.3 Local gradient, accumulation and net erosion

All regressions of site-average accumulation against site-average local gradient also gave comparatively poor results. The best fit was obtained using site-median local gradient in degrees ($r^2 = 0.515$ for topographic categories b, d and e, with N pins = 104; and $r^2 = 0.514$ for topographic categories d and e, with N pins = 85; both significant at 95%).

For site-average net erosion, best fits were obtained with site-average local gradient expressed as the Liu et al. (1994) and the Nearing (1997) S-factor variants: $r^2 = 0.802$ and $r^2 = 0.822$ respectively, with both significant at 99.9 % and having N pins = 158.

4. Discussion

Site-average local gradient proved to be an effective predictor of ground surface lowering, as measured by erosion pins, on the non-channel floor areas of our study sites.

From one point of view, this result merely confirms the obvious: that erosion rate has a strong dependence on gradient. There have been very few exceptions to this finding (one being the 1991 paper of Abrahams and Parsons, which found a different relationship on badland slopes with a coarse weathering mantle, for which stoniness increased with gradient). However from another point of view, our result is novel, since it relates to local gradient i.e. gradient at a point. This novelty is emphasised by the failure of more conventional measures of gradient to usefully predict erosion rates on each study site.

The value of our result is further highlighted when it is compared with other studies of between-site variability in erosion rate. Unfortunately, there are very few studies of variability of erosion rate on replicated plots on which soil loss has been measured using erosion pins. So comparisons with the current study are inevitably not wholly like-for-like. Soil loss on erosion plots is usually measured using a collection device at the foot of the plot. A value for soil loss obtained in this way is actually a value of sediment delivery from the plot, being a total for the whole area which ignores any within-plot deposition. By contrast, a value of soil loss derived from a grid of erosion pins only gives information regarding those pins at which erosion has occurred. This value may or may not be representative of erosion on the area between the pins, but it is independent of any pin-derived value for deposition. There are thus clear differences between erosion rates derived from conventional plots, and erosion rates derived from grids of erosion pins (cf. Sirvent et al., 1997; see also Section 4.3 below).

Despite this, it is still instructive to compare our result with other studies of replicate plots. A classic field study by Wendt et al. (1986) used 40 replicated conventional erosion plots. The authors concluded that “only minor amounts of observed variability could be attributed to any of several measured plot properties, and plot differences expressed by the 25 events did not persist in prior or subsequent runoff and soil-loss observations at the site”. Greater between-plot variability was associated with the least erosive storms. A study by

Nearing et al. (1999) analysed data from replicated pairs of conventional plots within the large USLE database: these authors also found considerable variability (coefficient of variability up to 15%) between replicates, irrespective of whether measurements were event, annual, or longer-term values. Again, variability decreased with greater total erosivity during the period of measurement. Results from these studies are discussed further below.

4.1 Local gradient, microrelief and emergent flow patterns

Why, then, is local gradient such a strong determinant of erosion on the non-channel floor portions of our study sites? Local gradient clearly has some relationship to within-site relief, since a complete absence of within-site relief would produce local gradients of zero. Similarly, a zero hillslope gradient would suggest zero, or very low, values of local gradient. However the three are not related in any simple way: compare the values of within-site relief and hillslope gradient in Table 2 with the distributions of local gradient in Figure 5.

Local gradient may also be considered from the perspective of slope curvature. Downslope curvature (i.e. slope shape) was shown, in a laboratory study by Reike-Zapp and Nearing (2005), to have a significant impact on runoff production, rill patterns, and sediment yield. 'Topographic curvature' (i.e. planform curvature) was shown by Heimsath et al. (1997) to be inversely correlated with soil thickness, and thus with the difference between erosion and soil production rates. However, the complex within-plot topography of our study sites means that slope curvature – whether downslope or planview – would, just as is the case with gradient and relief, be very difficult to capture objectively using only a single measure for each site. Downslope curvature is, nonetheless, implicit in multiple measurements of local gradient; but (as with gradient) the relationship between the two is not necessarily simple. Planform curvature is also implicit in each measurement of local gradient, but only if the orientation of each local gradient measurement is recorded.

The most fruitful approach is to consider a measurement of local gradient to be a sample of within-site topographic roughness (microrelief or rugosity), averaged over a horizontal length of a few cm (in our case, the length of the phone). This horizontal length scale is roughly intermediate between that of microrelief (mm), and that of relief on plot-sized areas (tens of cm to m).

The influence of microtopographic roughness on flow routing is the core concept underpinning the RillGrow soil erosion model (Favis-Mortlock, 1998). Given a DEM with a horizontal resolution of mm to cm, RillGrow is able to realistically reproduce observed rill networks (Favis-Mortlock et al., 2000). Other models of overland flow and erosion have employed the same concept (e.g. Darboux et al., 2002; Bursik et al., 2003; Ting et al., 2009). Experimental work (e.g. Gessesse et al., 2010) has also explored the link between microtopography and rill erosion: in particular, Bennett et al. (2015) experimentally demonstrated that the pre-rainfall pattern of microrelief is a strong determinant of the eventual planform pattern of rills. The average of measurements of local gradient on our study sites is therefore a powerful predictor of erosion rate for the same reason that a DEM of microtopography enables RillGrow to effectively predict observed rill networks: because variations in soil-surface elevation, on the scale of mm to cm, are what emergently determine the spatial pattern of overland flow, and hence the erosion produced by that flow.

It is therefore unsurprising – from two perspectives – that the best fit was obtained, for the site-average erosion vs site-average local gradient regressions, when measurements from pins with topographic category c (channel floor) were omitted.

The first perspective is that of self-organization (e.g. Phillips, 2011, 2014). It is the emergent patterns of flow on the pre-erosion microtopography of the soil's surface which dictate where rill incision begins. Once a rill has commenced incision, the channel develops its own talweg profile and its own within-channel roughness (Nearing et al., 1997). As the channel further incises, the talweg profile and the within-channel microrelief both become less and less related to the pre-erosion microtopography as the channel moves towards a state of minimum energy dissipation (Gomez et al., 2003). However overland flow continues to self-organize its routing on the inter-channel areas. Thus the channel areas and the inter-channel areas eventually form two distinct populations with regard to microtopography and local slope.

On the colluvium into which our study sites are incised, a unique pattern of microtopographic roughness developed at each site. The pattern of flow determined by microtopography then determined the spatial distribution of rills. Some rills eventually became gullies, and some gullies eventually cut down to bedrock. The gradients of the side slopes of the rills and gullies are therefore wholly independent of the original pre-erosion hillslope gradient, depending instead on runoff intensity and channel spacing. We have observed that, once a hillslope gully has cut to bedrock, the side slopes appear to evolve by a parallel retreat mechanism i.e. they maintain a constant slope angle: see also section 4.5. The along-interfluvial gradient is a relict of the original hillslope gradient. Nonetheless, the interfluvial areas are still erosionally active, having the highest value of net erosion and the second-highest value of erosion.

The second perspective concerns flow depth and erosion sub-processes during runoff events. In the channels, the maximum flow depth that has been observed is a few cm; for every other topographic category, flow depth never exceeds a few mm. Using the terminology of Kinnell (2005), the shallow flow on the inter-channel areas will experience raindrop detachment with transport by raindrop splash (RD-ST), raindrop detachment with transport by raindrop-induced flow transport (RD-RIFT), and possibly raindrop detachment with transport by flow (RD-FT). However the deeper and faster flow in the channels will additionally give rise to flow detachment with transport by flow (FD-FT), which will dominate in the most energetic flows. Thus the channel and inter-channel areas again form two distinct populations, but this time with each population based on a set of erosional sub-processes.

To summarize and generalize: when any previously uneroded site begins to erode, its initial microtopography (derived from the pre-erosion colluvium surface) determines the pattern of flow routing, which in turn determines the site's initial rate and spatial pattern of erosion, and the eventual location of rills and gullies. Since the microrelief of every site is different, there may be considerable between-site variability in erosion rate. At this stage, the average of all measurements of local gradient taken at any point on the site will correlate strongly with erosion rate on that site i.e. all local gradient measurements are part of a single statistical population. However, as the site erodes further, the proportion of its area occupied by channels increases. Channels create their own microtopography which is distinct from that of the inter-channel areas, but which is similar to that of other channels. Thus local gradient measurements from points in topographic category c (channel floor) form a distinct population, one which relates only weakly to soil loss as measured by erosion pins. But local gradient measurements from all other topographic

categories form a different statistical population. This population possesses an average value which correlates strongly with soil loss as measured by erosion pins.

This perspective is illuminating with respect to the previously-discussed results of Wendt et al. (1986) and Nearing et al. (1999) who both found that the difference between replicates decreased as the magnitude of measured soil loss increased. With all else being equal, an erosion plot which has suffered more erosion will have developed more (and/or larger) rills than a plot which has eroded less. So the more-eroded replicates have a greater proportion of their area occupied by channels, and a correspondingly smaller proportion which is inter-channel. The variability of microtopography – and hence of soil loss – is greater on inter-channel areas, and lower on channelled areas. Thus the variability of erosion rate is greater on less-eroded replicates which have fewer (and/or smaller) rills, and lower on more-eroded replicates which have more (and/or larger) rills. It is interesting to speculate whether, if the data used in the studies of Wendt et al. (1986) and Nearing et al. (1999) had included records of the proportion of each plot's area occupied by rills, this would have helped to explain the between-replicate differences.

4.2 Local gradient, accumulation, and net erosion

By contrast, all our regressions between accumulation rate and site-averaged local gradient gave relatively poor results. This suggests that accumulation on these sites is driven by processes which are generally unrelated to microtopography and the routing of overland flow. This is to be expected for weathering processes such as wetting and drying. The best fit for accumulation ($r^2 = 0.515$, significant at 95%, N pins = 104) was obtained with the median of measurements of local gradients in degrees, from topographic categories b, d and e.

Regressions using net erosion gave the best result ($r^2 = 0.822$, N pins = 158, topographic categories a, b, d and e) when the more sophisticated USLE-based transformation by Nearing (1997) was used. It is interesting to speculate on the reason for this. The USLE was developed to estimate average annual soil loss from an erosion plot (Wischmeier and Smith, 1978), but only from that part of the plot which has experienced net soil loss (Nearing, 2013). Net erosion (erosion minus accumulation at each pin) on our sites is not exactly the same as this; but it may be sufficiently similar that the USLE-based transformations of local slope are better suited to predict net erosion, and hence give the best fit when net erosion is regressed against USLE-based transformations of site-averaged local slope.

4.3 Local gradient and sediment delivery

Throughout this paper we have been confined to considering only erosion as measured by change of exposure at 25 erosion pins on each study site. The relationships between site-average local gradient and erosion on the whole area of each site remains unknown, as does the relationship between site-average local gradient and sediment delivery from each site. There appears to be little consensus regarding comparative rates measured by erosion pins and by collector devices (Sirvent et al., 1997). We, unfortunately, do not have measurements for runoff and sediment leaving each site. Given the remoteness and consequent difficulty of regular monitoring of collector devices, it is unlikely that direct measurements of runoff and sediment export will be obtained for our study sites. However, some inferences are possible. Observations suggest that erosion pins on interfluvies and side slopes rarely produce accumulation: this implies a sediment delivery ratio close to unity for such pins.

4.4 Temporal change in local gradient

A possible major limitation of this study derives from the measurements of local gradient being made after, rather than before, the measurements of erosion and accumulation. The latter were made over a period of many years. During this time, changes in ground-surface elevation due to erosion and accumulation will certainly have had some impact upon local gradients. Thus we are effectively comparing erosion rates with the local gradients produced by erosion, rather than comparing erosion with the local gradients which gave rise to that erosion.

We have no visual evidence of major changes in local gradient at the majority of erosion pins. This being so, the difference between pre-erosion and post-erosion local gradient is probably too small to have significantly compromised our results. But larger changes in local gradient are known to have occurred for a minority of pins; most of which, however, have been omitted from our analysis for the following reasons.

- When measuring change in pin exposure, some pins were found to have been moved from their correct position in the grid. This might result from vertical or near-vertical sidewall collapse. No results are recorded for such a pin; the pin is then re-inserted in its correct position in the grid (Boardman and Favis-Mortlock, 2016). These ‘lost pin’ measurements occur infrequently, for only c. 5% of pin measurements (see Table 3 in Boardman et al., 2016).
- A pin may be found to have changed its topographic category. Such pins were excluded from the regression analysis (see Section 3.1).
- A third situation in which local gradient could change notably is when temporary accumulation of colluvium occurs, prior to channel scour. However, this can occur only in topographic category c (channel floor). Pins with this category were omitted from the best-fit regression shown in Figure 7.

As an additional check, we explored the relationship between pre-erosion and post-erosion local gradient using a simple Python script. This simulates, in cross section, the erosion of a channel. Starting with an initially flat surface (the horizontal line in the upper graph of Figure 9) incised by a single nick, flow along the channel (i.e. in to or out of the plane of the Figure) deepens the channel at a fixed rate which does not depend on local slope. Points at which this along-channel lowering occurs are indicated by a thicker line on each cross section, and correspond to topographic category c (channel floor). However, erosional lowering elsewhere on each cross section (thinner lines) is dependent on local gradient: this corresponds to all other topographic categories. In the model, erosion proceeds iteratively, with the cross section created at the end of one timestep becoming, after some smoothing to remove artefacts, the cross section for the next timestep. After 500 timesteps a roughly U-shaped channel is developed.

The lower graph in Figure 9 shows the relationship between average local gradient and depth of soil lost, for all non-channel floor points on each cross section. The solid line relates the average local gradient at the start of each timestep with soil lost during that timestep. The dashed line relates the average local gradient at the end of each timestep with soil lost during that timestep. The two lines differ little: the difference is slightly greater at the beginning of the simulation. The relationship is close to linear during the second half of the simulation, less so during the first half.

This simple simulation of course omits several important aspects of erosional behaviour at the study sites (for example: sidewall collapse, lowering of the interfluves as rills and

gullies widen, the influence of bedrock) but it does show that change in average local gradient on the non channel floor areas is fastest during the early stages of channel incision. Once a channel has been established, average local gradient on the non channel floor areas changes only slowly. This indicates that our use of pre-erosion average local gradient is not a problem.

Simulations of rill initiation and development using RillGrow also show similar behaviour, with changes in microtopographic slope being fastest in the earliest stages of rill incision (Favis-Mortlock et al., 2000). Once channels have been established, change in channel-side local gradient becomes slower. As channels develop further, as can be seen in the later cross sections in the upper graph of Figure 9, the retreat of channel sidewalls is close to parallel.

4.5 Erosional history of the study sites

These results have implications for the erosional history of our study sites. The initial phase was one of channel downcutting into what (we assume) was a relatively uniform initial thickness of colluvium, deposited upon a pre-existing topography. At this stage, average local gradient changed relatively rapidly. As channels became more established, average local gradient changed more slowly. Eventually, some channels reached sub-colluvial bedrock, with others close to bedrock. Currently, erosion on our study sites is dominated by largely stable average local gradient, with parallel retreat of channel side slopes, and concomitant narrowing (and eventual removal) of interfluves. The hillslope gradient, which is still to some extent preserved as the along-interfluve gradient, is now a historic feature that has only a minor role in influencing what is happening on these badland sites. It is therefore unsurprising that hillslope gradient (see Table 2 and section 1.5 above) proved to be an ineffective predictor of present-day erosion.

***** TABLE 5**

From the average rate of net lowering and the average local slope for each topographic category, and by assuming parallel retreat of channel side slopes, it is possible to calculate the rate of horizontal retreat of channel sidewalls (Table 5). If between-channel spacing is 3 m, then the interfluves (assuming no interfluve lowering) will be eroded away in 3-5 k years. However this is an overestimate, since the interfluve areas are still experiencing erosion.

4.6 Sensitivity analysis

Finally, we carried out a sensitivity analysis of the main finding of this paper by replicating the regression shown in Figure 7 with pins randomly removed. Removal of a pin means that the measurement of local gradient at that pin, and the value of long-term erosion at that pin, is ignored. The dashed line in Figure 10 shows the mean r^2 of each set of 1000 replicates, each set having had the same number of pins removed from each site. The whiskers indicate that the 'predictive power' of individual pin measurements varies greatly. Removal of some pin measurements dramatically decreased the correlation; removal of others had little effect. Naively, it might be expected that removal of pin measurements from each site would lower the correlation linearly. So the removal of one pin measurement from each of the ten sites would lower the r^2 value by $1/25$, removal of two pin measurements would lower it by $2/25$, etc. The dotted line shows the r^2 values which result from this 'naive assumption'. The dashed line decreases more steeply. i.e. removal of pin measurements causes, on average, a steeper decline in predictive power than does this 'naive assumption'.

These results are again consistent with the notion that flow routing on the inter-channel areas of the sites forms an emergent system. Some pins are located in areas which, due to the vagaries of microrelief, convey a greater proportion of overland flow. Measurements at these pins may well also convey a greater-than-expected share of information about erosion at adjacent pins, and (by extension) on the whole site. For other pins the converse is true. This spatial pattern of flow and erosion on the non-channel areas of our sites is an example of 'weak emergence' (Bar-Yam, 1997): the behaviour of the emergent system is perturbed, but only in a relatively minor way, by random interference with its components.

A multiple regression using the results from this sensitivity analysis yielded the following equation ($r^2 = 0.571$, significant at 95%):

$$r_squared = (0.0069 * n_pins) - (0.0039 * percent_a) + (0.0029 * percent_b) - (0.0008 * percent_d) - (0.0099 * percent_e)$$

where percent_a is the percentage of replicates which include topographic category a, etc. This result indicates that the ability of site-average local gradient to predict erosion is enhanced by including measurements from a larger number of pins, and by the inclusion of a greater fraction of pin measurements from topographic category b (very steep or vertical channel side wall). By contrast, the ability of site-average local gradient to predict erosion tends to lessen if a greater fraction of pin measurements from topographic categories e (narrow interfluvium between channels), a (broad flat interfluvium), and to a much lesser extent d (footslope), are included. The implication is that a greater share of erosional information is contributed by pin measurements made on very steep or vertical channel side wall areas, and a lesser share of information is contributed by pin measurements made on interfluviums.

4.7 Further work

As in any measurement, there is some error in our measurements of local gradient. This will have been introduced mainly when choosing the direction of greatest slope, and hence the orientation of the local gradient measurement. A limited number of replicate tests suggest that this error is small, less than one degree. Boardman et al. (2015) and Boardman and Favis-Mortlock (2016) describe a procedure which was used to quantify error when taking measurements of change in erosion pin exposure. A similar exercise will be carried out to quantify errors in local gradient measurements. We also intend to record the orientation of local gradient in future studies.

The values for infiltration presented in Table 2 are questionable, in part because measurements made using portable mini-disc infiltrometers are liable to be influenced by local variability in soil properties. We plan to use a rainfall simulator to obtain infiltration measurements over a larger area. The rainfall simulation experiments will also permit indirect estimates of runoff and sediment export from the study sites.

For each site, the pattern of channels established on the pre-incision colluvial surface will have been controlled by the microrelief of that surface. However the spacing of these channels will also, to some extent, be dependent on the overall gradient of this pre-incision surface, the 'hillslope gradient'. Thus sites with similar hillslope gradients may show similarities in channel spacing. This is to be followed up by systematically measuring channel spacing.

Finally, whilst it is encouraging to have discovered a strong link between erosion rate and site-average local gradient on the non-channel portions of our sites, it must be remembered that erosion rates have been measured using erosion pins. We do not know

whether any relationship exists between erosion rate measured using some other approach, and site-average local gradient on the non-channel portions of a site. It would be of great interest to test this on better-instrumented sites, both in badland locations and elsewhere.

5. Conclusions

Site-average values of local gradient, defined as the steepest slope angle measured at an erosion pin, are a powerful predictor of long-term rates of soil loss as measured by erosion pins on the non-channel floor portions of ten badland study sites in the Karoo area of South Africa. Local gradient may be easily measured using a smartphone clinometer. The successful use of local gradient here is in strong contrast to the previous failure of several other site-specific attributes, including other measures of gradient and relief, to explain between-site variation in erosion rate on these study sites. However, the predictive ability of site-average local gradient for more conventional erosion plots, on which soil loss is measured by a collector device, is still unknown.

A measurement of local gradient may be thought of as a sample of a site's microtopography. Microrelief is a strong determinant of the emergent patterns of inter-channel overland flow, and hence of the patterns of inter-channel erosion by flow. This explains the success of site-average local gradient as a predictor of erosion on the non-channel floor portions of the study sites. The microtopography of the channel floor areas constitutes a separate population.

Local gradient changes most rapidly during the initial stages of channel incision. When channels are established, local gradient changes more slowly leading to almost-parallel retreat of channel sidewalls. This has implications for the erosional history of our study sites: following initial incision of channels down the original 'hillslope gradient', considerable within-site relief developed. This relief now dominates erosion on the sites: the hillslope gradient has become a relict feature with little relevance to present-day erosion.

A sensitivity analysis suggests that not all individual measurements of local gradient are equal with regard to prediction of long-term erosion rate. Removal of measurements at some pins had little effect, whilst removal of others greatly weakened the correlation. A greater share of predictive power is contributed by measurements made on very steep or vertical channel side wall areas, and a lesser share is contributed by measurements made on interfluves.

Acknowledgements

Many people over the years have assisted with data collection on the badland erosion sites, in particular, we thank Professor Kate Rowntree for help with the clinometer measurements. The badland sites are on land owned by Ms Shauna Westcott and Alf and Brenda James: we thank them for hospitality and willing co-operation. Finally, we thank the anonymous reviewers and the Associate Editor: both for their insightful and very helpful comments on an earlier version of this paper, and for their thought-provoking (but currently unanswerable) questions.

The Python scripts used to analyse the data and to produce the graphs may be downloaded from http://soilerosion.net/dfm/espl_karoo_2017/.

References

- Abrahams, A.D. and Parsons, A.J. 1991. Relation between sediment yield and gradient on debris-covered hillslopes, Walnut Gulch, Arizona. *Geological Society of America, Bulletin* 103, 1109-1113
- Bar-Yam, Y. 1997. *Dynamics of Complex Systems*. Perseus Books, New York, USA
- Bennett, S.J, Gordon, L.M, Neroni, V. and Wells, R.R. 2015. Emergence, persistence, and organization of rill networks on a soil-mantled experimental landscape. *Natural Hazards* 79(1), 7-24
- Boardman J, Parsons AJ, Holmes PJ, Holland R, Washington R. 2003. Development of badlands and gullies in the Sneeuberg, Great Karoo, South Africa. *Catena* 50 (2-4): 165-184
- Boardman, J., Holmes, P.J., Rhodes, E.J., and Bateman, M.D. 2005. Colluvial fan gravels, depositional environments and luminescence dating: a Karoo case study. *South African Geographical Journal* 87(1), 73-79
- Boardman, J, Foster, I.D.L, Rowntree, K, Favis-Mortlock, D, Suich, H. and Gaynor, D. 2017. Long-term studies of land degradation in the Sneeuberg uplands, eastern Karoo, South Africa: a synthesis. *Geomorphology* 10.1016/j.geomorph.2017.01.024
- Boardman, J, Favis-Mortlock, D.T. and Foster I.D.L. 2015. A 13-year record of erosion on badland sites in the Karoo, South Africa. *Earth Surface Processes and Landforms* 40, 1964-1981 DOI: 10.1002/esp.3775
- Boardman, J. and Favis-Mortlock, D.T. 2016. The use of erosion pins in geomorphology. Chapter 3.5.3 in Cook, S.J., Clarke, L.E. and Nield, J.M. (Eds) *Geomorphological Techniques (Online Edition)*. British Society for Geomorphology, London, UK
- Bursik, M, Martínez-Hackert, B, Delgado, H. and Gonzalez-Huesca, A. 2003. A smoothed-particle hydrodynamic automaton of landform degradation by overland flow. *Geomorphology* 53(1–2), 25–44
- Darboux, F, Gascuel-Odoux, C. and Davy, P. 2002. Effects of surface water storage by soil roughness on overland-flow generation. *Earth Surface Processes and Landforms* 27(3), 223–233
- De Ploey, J. and Savat, J. 1968. Contribution a l'étude de l'érosion par le splash, *Zeitschrift für Geomorphologie* 12, 174-193
- Favis-Mortlock, D.T. 1998. A self-organising dynamic systems approach to the simulation of rill initiation and development on hillslopes. *Computers and Geosciences* 24(4), 353-372
- Favis-Mortlock, D.T, Boardman, J, Parsons, A.J. and Lascelles, B. 2000. Emergence and erosion: a model for rill initiation and development. *Hydrological Processes* 14(11-12), 2173-2205
- Foster, I.D.L., Boardman, J., and Keay-Bright, J. 2007. Sediment tracing and environmental history for two small catchments, Karoo uplands, South Africa. *Geomorphology* 90, 126-143

- Gessesse, G.D, Fuchs, H, Mansberger, R, Klik, A. and Rieke-Zapp, D.H. 2010. Assessment of erosion, deposition and rill development on irregular soil surfaces using close range digital photogrammetry. *The Photogrammetric Record* 25(131), 299–318
- Gilbert, G.K. 1877. *Report on the geology of the Henry Mountains*. US Geographical and Geological Survey, Washington DC, USA. 160 pp
- Gomez, J.A., Darboux, F. and Nearing, M.A. 2003. Development of rill networks under simulated rainfall: evolution towards a state of minimum rate of energy dissipation. *Water Resources Research* 39(6), 1148
- Heimsath A.M, Dietrich, W.E, Nishiizumi, K. and Finkel R.C. 1997. The soil production function and landscape equilibrium. *Nature* 388, 358–361
- Holmes, P.J., Boardman, J., Parsons, A.J., and Marker, M.E. 2003. Geomorphological palaeoenvironments of the Sneeuwberg Range, Great Karoo, South Africa. *Journal of Quaternary Science* 18(8), 801-813
- Keay-Bright, J. and Boardman, J. 2009. Evidence from field based studies of rates of erosion on degraded land in the central Karoo, South Africa. *Geomorphology* 103, 455-465
- Kinnell, P.I.A. 2005. Raindrop-impact-induced erosion processes and prediction: a review. *Hydrological Processes* 19, 2815-2844
- Liu, B.Y, Nearing, M.A. and Risse, L.M. 1994. Slope gradient effects on soil loss for steep slopes. *Transactions of the American Society of Agricultural Engineering* 37(6), 1835–1840
- Nearing, M.A. 1997. A single, continuous function for slope steepness influence on soil loss. *Soil Science Society of America Journal* 61, 917-919
- Nearing, M.A, Norton, L.D, Bulgakov, D.A, Larionov, G.A, West, L.T. and Dontsova, K.M. 1997. Hydraulics and erosion in eroding rills. *Water Resources Research* 33(4), 865-876
- Nearing, M.A, Govers, G. and Norton, L.D. 1999. Variability in soil erosion data from replicated plots. *Soil Science Society of America Journal* 63(6), 1829–35
- Nearing, M.A. 2013. Soil Erosion and Conservation. In Wainwright, J. and Mulligan, M. (eds) *Environmental Modelling: Finding Simplicity in Complexity*, 2nd Edition. Wiley, UK, 365-378
- Phillips, J.D. 2014. Thresholds, mode switching, and emergent equilibrium in geomorphic systems. *Earth Surface Processes and Landforms* 39, 71–79
- Phillips, J.D. 2011. Emergence and pseudo-equilibrium in geomorphology. *Geomorphology* 132, 319–326
- Rieke-Zapp, D.H, and Nearing, M.A. 2005. Slope shape effects on erosion. *Soil Science Society of America Journal* 69(5), 1463-1471
- Sirvent J, Desir G, Gutierrez M, Sancho C. and Benito G. 1997. Erosion rates in badland areas recorded by collectors, erosion pins and profilometer techniques (Ebro basin, NE-Spain). *Geomorphology* 18: 61-75
- Ting, M.A, Zhou, C.-H. and Cai, Q.-G. 2009. Modeling of hillslope runoff and soil erosion at rainfall events using cellular automata approach. *Pedosphere* 19(6), 711-718

Wendt, R.C, Alberts, E.E. and Hjelmfelt, A.T. Jr. 1986. Variability of runoff and soil loss from fallow experimental plots. *Soil Science Society of America Journal* 50, 730–6

Wischmeier, W.H and Smith, D.D. 1978. *Predicting rainfall erosion losses: a guide to conservation planning*. USDA Agricultural handbook 537, US Department of Agriculture, Washington DC, USA

Site Name	Site Code	Grid Size (m)	Duration of Measurement (years)	Average Erosion (mm yr ⁻¹)	Average Accumulation (mm yr ⁻¹)	Average Net Erosion (mm yr ⁻¹)
Good Hope 1	GH1	8 x 4	15.68	5.8 ± 0.3	2.6 ± 0.2	3.2 ± 0.5
Good Hope 2	GH2	8 x 4	15.68	8.1 ± 0.5	4.4 ± 0.4	3.7 ± 0.9
Compassberg 1	C1	8 x 4	15.67	7.2 ± 0.5	3.2 ± 0.3	4.0 ± 0.8
Compassberg 2	C2	8 x 4	15.67	11.5 ± 0.7	4.5 ± 0.6	7.0 ± 1.3
Oppermanskraal 1	O1	4 x 4	14.94	8.6 ± 0.6	2.4 ± 0.4	6.2 ± 0.9
Oppermanskraal 2	O2	4 x 4	14.75	5.9 ± 0.3	1.3 ± 0.1	4.6 ± 0.4
Low Upper Oppermanskraal	LUO	4 x 4	14.75	6.2 ± 0.4	3.1 ± 0.4	3.1 ± 0.8
Up Upper Oppermanskraal	UUO	4 x 4	14.75	7.1 ± 0.4	4.9 ± 0.5	2.2 ± 1.0
Lower Lucernvale	LL	4 x 4	14.74	8.5 ± 0.5	1.9 ± 0.3	6.6 ± 0.8
Upper Lucernvale	UL	4 x 4	14.74	9.4 ± 0.5	1.4 ± 0.2	7.9 ± 0.6

Table 1. The ten erosion study sites. Results up to November 2016

Site Code	Average Erosion (mm yr ⁻¹)	Elevation (m)	Hillslope Gradient (%)	Aspect (deg.)	Within-Site Relief (m)	Bedrock in channels?	Sand (%)	Specific Surface Area (g m ⁻²)	Bulk density (g cm ⁻³)	Aggregate Stability (% stable, 0.5-2 mm)	Infiltration (mm hr ⁻¹)
GH1	5.8	1698	7.0	100	0.6	Y	26	1.104	1.63	71.5	54.4
GH2	8.1	1702	7.0	110	1.8	N	24	0.996	1.69	69.4	44.4
C1	7.2	1728	3.5	30	0.9	Y	23	0.982	1.51	71.2	8.0
C2	11.5	1732	3.5	0	1.5	Y	28	1.006	1.66	76.6	32.2
O1	8.6	1703	15.8	80	0.8	N	36	0.912	1.86	32.1	36.0
O2	5.9	1710	10.5	120	1.0	N	36	0.917	1.76	60.4	28.4
LUO	6.2	1750	7.0	20	1.2	N	28	0.803	1.73	38.3	22.2
UUO	7.1	1755	7.0	40	0.7	N	25	0.964	1.63	40.4	13.6
LL	8.5	1713	4.4	0	0.8	N	22	0.900	1.58	60.3	44.5
UL	9.4	1735	17.6	0	1.5	N	30	0.986	1.76	57.0	22.2

Table 2. Attributes of the erosion pin sites which showed little relationship with long-term average erosion for each plot. The same attributes also showed little relationship with net erosion, the percentage of eroding pins on each plot, and the ratio of long-term erosion to long-term accumulation, on each site. The infiltration rates were made using portable mini-disc infiltrometers. These are surprisingly high, despite being the mean of multiple measurements: measurement problems (including the difficulty of using the infiltrometer on steep slopes, and the impact of small-scale soil features such as cracking) may well have inflated these values

	Site Code		Topographic Category					Total
			a	b	c	d	e	
Percentage of All Valid Pin Measurements	GH1	N = 534	28.9	0.7	27.9	42.5	0.0	100
	GH2	N = 521	8.8	12.1	27.1	51.6	0.4	100
	C1	N = 459	34.6	6.3	24.0	29.6	5.5	100
	C2	N = 439	16.2	8.2	32.1	35.5	8.0	100
	O1	N = 440	27.0	28.4	20.7	15.0	8.9	100
	O2	N = 410	43.9	7.6	13.6	31.5	3.4	100
	LUO	N = 427	20.7	4.9	15.9	58.5	0.0	100
	UUO	N = 445	20.0	5.6	16.6	53.8	4.0	100
	LL	N = 420	19.8	5.2	25.7	49.3	0.0	100
	UL	N = 428	40.2	21.0	11.2	27.6	0.0	100
	Mean		26.0	10.0	21.5	39.5	3.0	
Average Erosion (mm yr⁻¹)	GH1		1.52	0.02	2.10	2.18		5.8
	GH2		0.88	1.33	2.14	3.64	0.08	8.1
	C1		2.73	0.59	1.76	1.56	0.57	7.2
	C2		2.30	1.10	4.22	2.68	1.24	11.5
	O1		1.87	3.61	1.14	1.14	0.88	8.6
	O2		2.39	0.58	0.63	1.98	0.34	5.9
	LUO		1.85	0.37	0.86	3.08		6.2
	UUO		1.58	0.32	1.43	3.46	0.32	7.1
	LL		1.36	0.50	2.36	4.28		8.5
	UL		3.10	2.76	0.52	2.98		9.4
	Mean		1.96	1.12	1.72	2.70	0.57	
Standard Deviation		0.67	1.17	1.09	0.98	0.42		
Average Accumulation (mm yr⁻¹)	GH1		0.33	0.03	1.28	0.96		2.6
	GH2		0.18	0.17	2.33	1.71	0.01	4.4
	C1		0.26	0.05	1.53	1.31	0.07	3.2
	C2		0.39	0.05	2.72	1.34	0.00	4.5
	O1		0.25	0.22	1.51	0.39	0.04	2.4
	O2		0.21	0.13	0.51	0.43	0.00	1.3

	LUO	0.14	0.04	1.28	1.64		3.1	
	UO	0.19	0.17	2.47	2.04	0.02	4.9	
	LL	0.16	0.01	0.84	0.86		1.9	
	UL	0.49	0.27	0.46	0.22		1.4	
	Mean	0.26	0.11	1.49	1.09	0.02		
	Standard Deviation	0.11	0.09	0.80	0.62	0.03		
Average Net Erosion (mm yr⁻¹)	GH1	1.18	-0.01	0.82	1.22		3.2	
	GH2	0.70	1.16	-0.19	1.93	0.08	3.7	
	C1	2.47	0.55	0.22	0.26	0.50	4.0	
	C2	1.91	1.05	1.50	1.34	1.24	7.0	
	O1	1.62	3.39	-0.37	0.74	0.84	6.2	
	O2	2.18	0.46	0.12	1.55	0.34	4.7	
	LUO	1.71	0.33	-0.42	1.44		3.1	
	UO	1.39	0.15	-1.04	1.43	0.30	2.2	
	LL	1.21	0.50	1.52	3.42		6.7	
	UL	2.61	2.49	0.07	2.76		7.9	
		Mean	1.70	1.01	0.22	1.61	0.55	
		Standard Deviation	0.61	1.10	0.83	0.92	0.42	

Table 3. The percentage of all valid pin measurements, and average rates of erosion, accumulation and net erosion, for each of the five topographic categories at the ten study sites. Erosion, accumulation and net erosion rates are averages for the whole pin grid (i.e. all 25 pins) and sum to the values for all topographic categories shown in Table 1

Significance (%)	Topographic categories	r²	N pins
99.99	a b d e	0.918	158
99.9	a b c d	0.839	182
	a b c d e	0.824	189
	a b d	0.789	151
	a b c	0.769	104
	d	0.764	78
99	b c d e	0.746	135
	d e	0.742	85
	b c d	0.727	128
	a d	0.695	132
	a b c e	0.695	111
	b d e	0.689	104
	a b	0.637	73
	a d e	0.613	139
	a b e	0.591	80
95	c d	0.555	109
	a c d	0.483	163
	c d e	0.480	116
	b d	0.458	97
	b c e	0.431	57
	a c d e	0.429	170
	b c	0.419	50
Not significant	a e	0.136	61
	e	0.115	7
	a c	0.111	85
	b e	0.111	26
	a c e	0.042	54

Significance (%)	Topographic categories	r²	N pins
	a	0.105	92
	b	0.001	19
	c	0.017	31
	c e	0.000	38

Table 4. Regression results for site-average erosion rate vs site-average local gradient, in decreasing order of significance and r²

Topographic category	Average local gradient (degrees)	Long-term average net erosion (mm yr⁻¹)	Horizontal retreat (mm yr⁻¹)
b	42	1.01	0.9
d	20	1.61	0.6

Table 5. Long-term average rate of horizontal retreat for two topographic categories, assuming parallel retreat

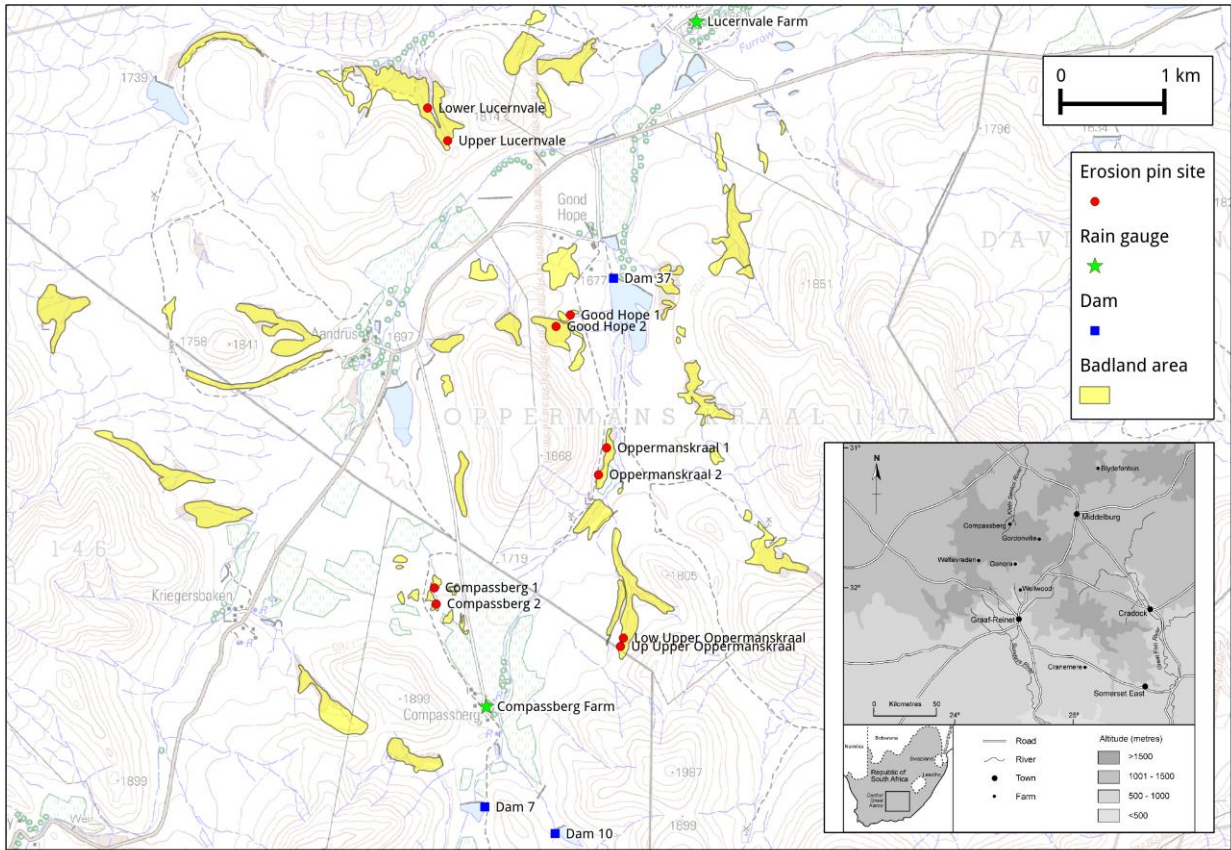


Figure 1. Location of the study area, erosion pin sites, raingauges and badland areas. From Boardman et al. 2015



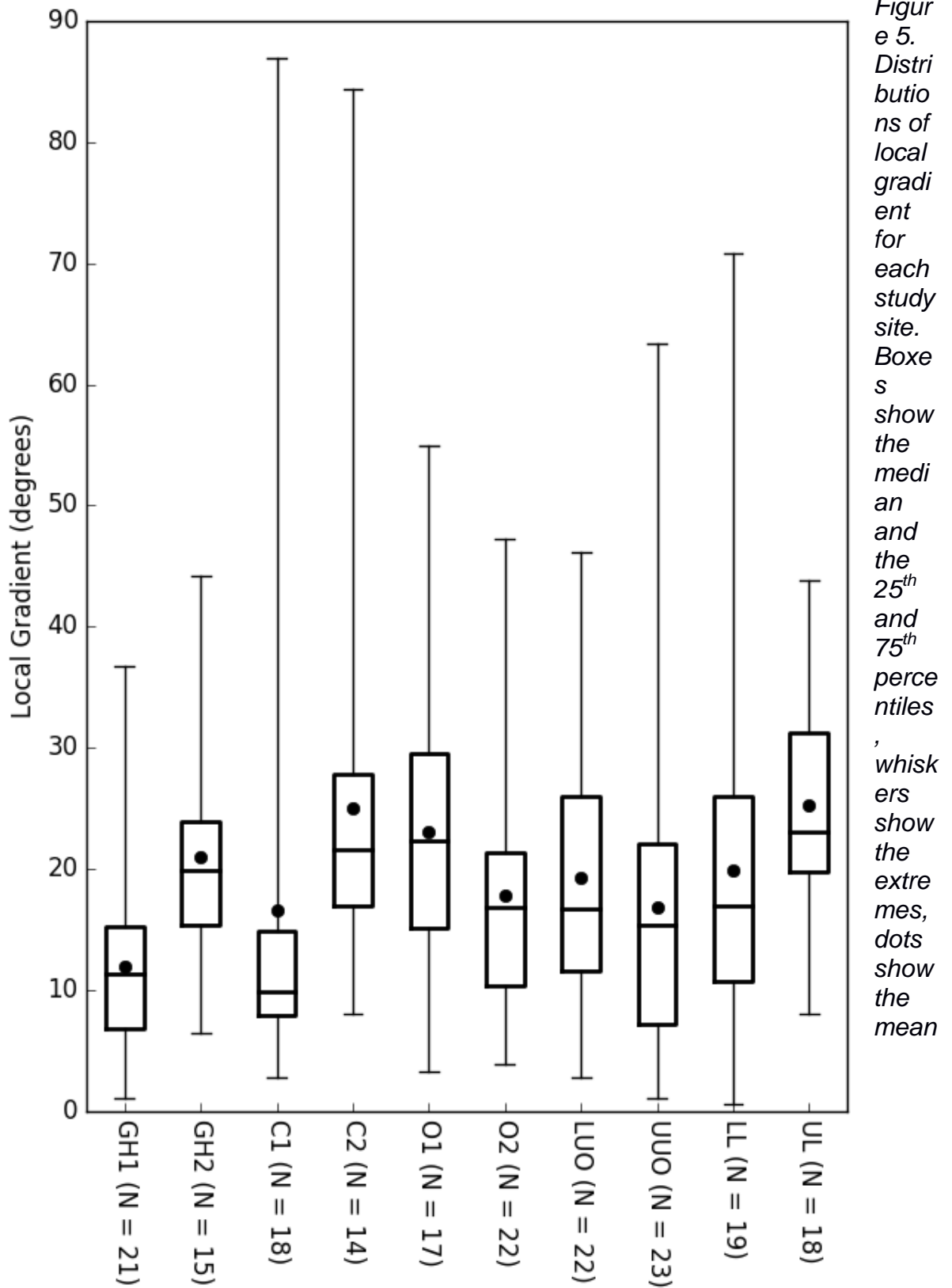
Figure 2. Runoff at the C1 site, taken in light rain in early 2004. Video footage of runoff from other locations in the study area is also available (see http://soilerosion.net/dfm/espl_karoo_2017/)



Figure 3. The C1 site, showing erosion pins and examples of the topographic categories



Figure 4. Using the clinometer app. The long axis of the phone is 13 cm



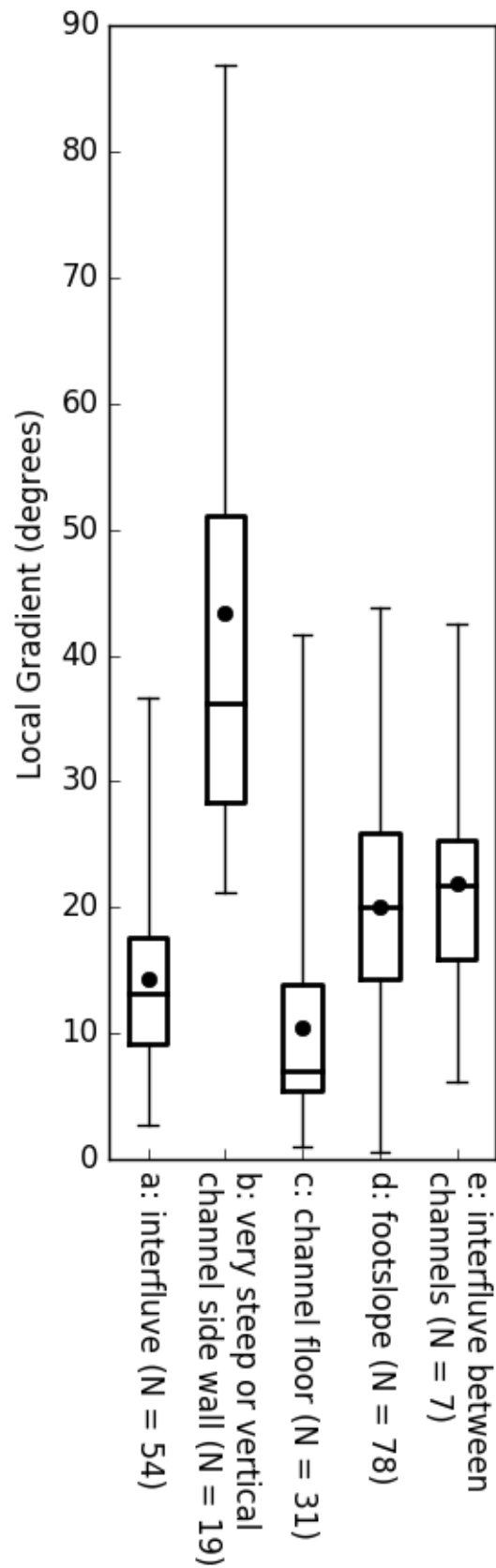


Figure 6. Distributions of local gradient for each topographic category. Boxes show the median and the 25th and 75th percentiles, whiskers show the extremes, dots show the mean

**Topographic Categories a b d e:
Site-Average Erosion vs Site-Average Local Gradient**

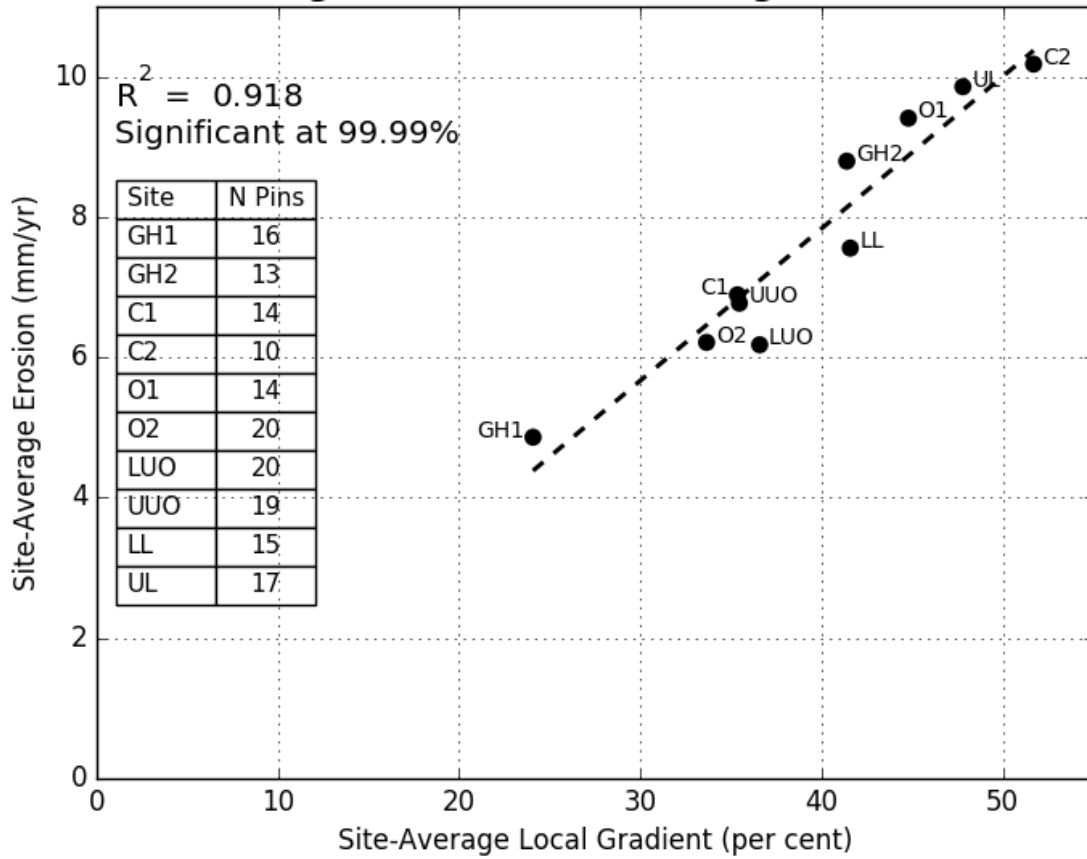


Figure 7. Site-average erosion rate v. site-average local gradient for each study site, for topographic categories a, b, d, e

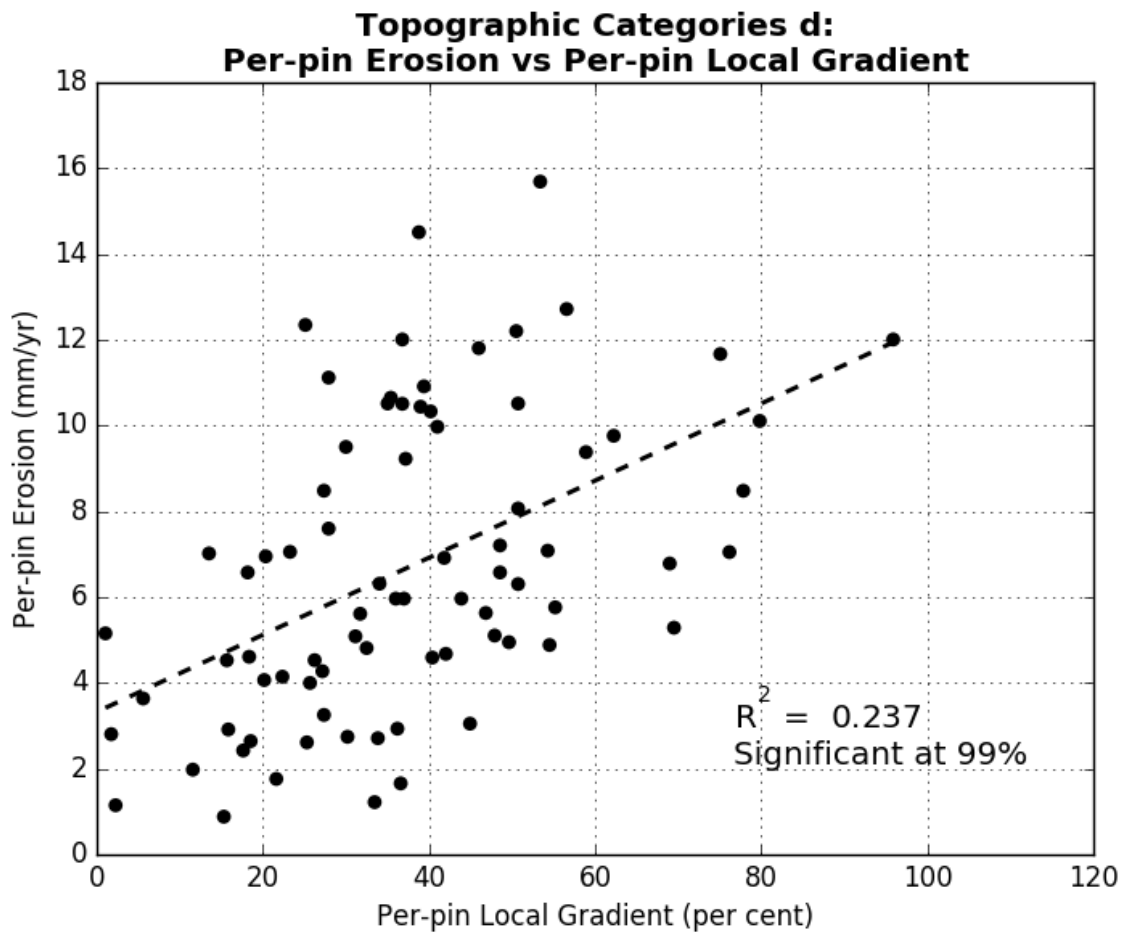


Figure 8. Per-pin erosion rate v. per-pin local gradient for all study sites, for topographic category d

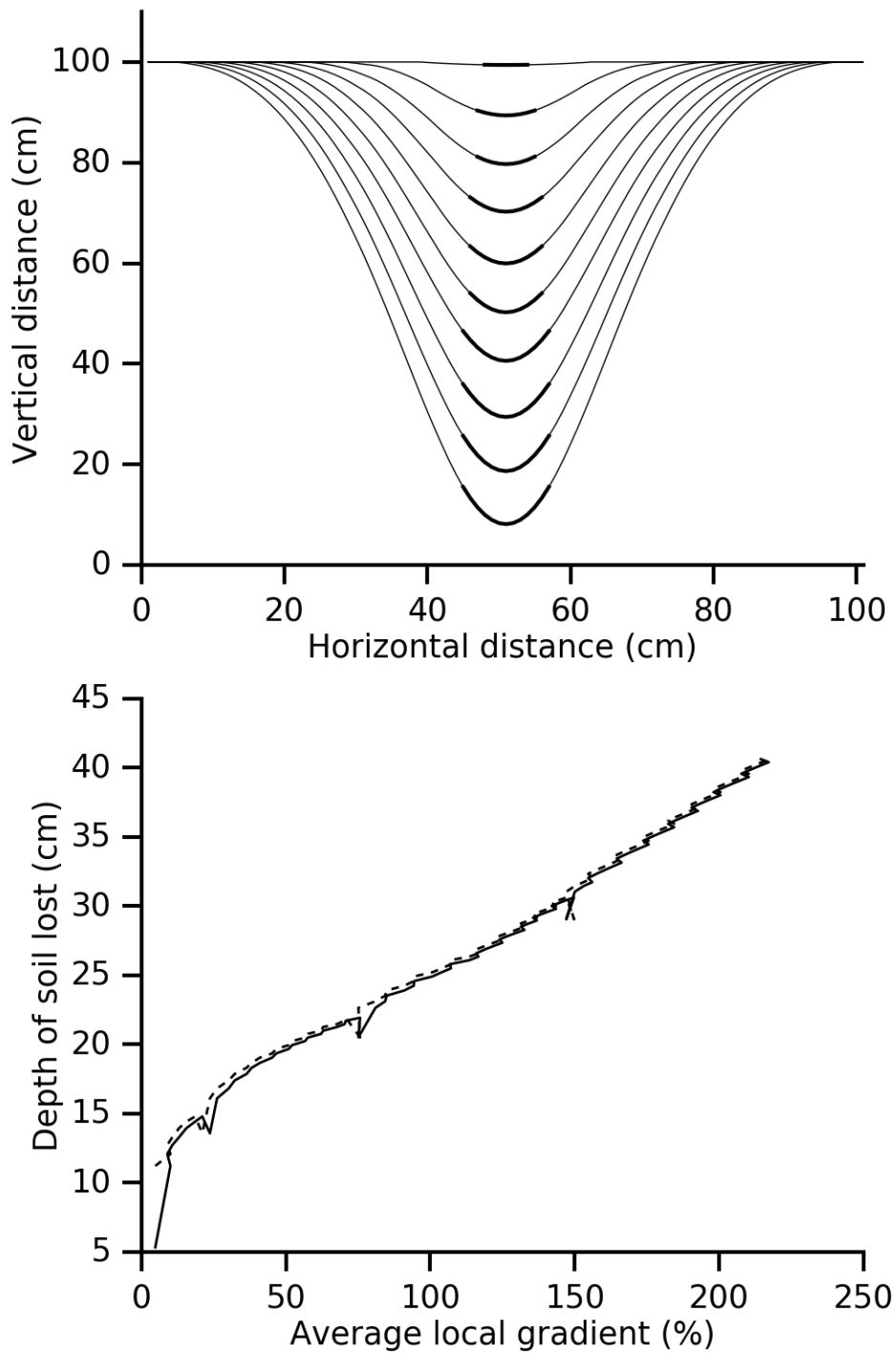


Figure 9. The simulated development of a channel, in cross section, from an initially horizontal surface incised by a single nick (upper graph). Channel flow is in to or out of the plane of the graph. Erosional lowering due to channel flow (thick line) is unrelated to local gradient, however erosional lowering elsewhere on the cross section (thin line) is related to local gradient. A cross section is shown only for every tenth timestep. The lower graph shows, for the non channel part of each cross section, the relationship between depth of soil lost during each timestep, and average local gradient before (dashed line) and after (solid line) that timestep

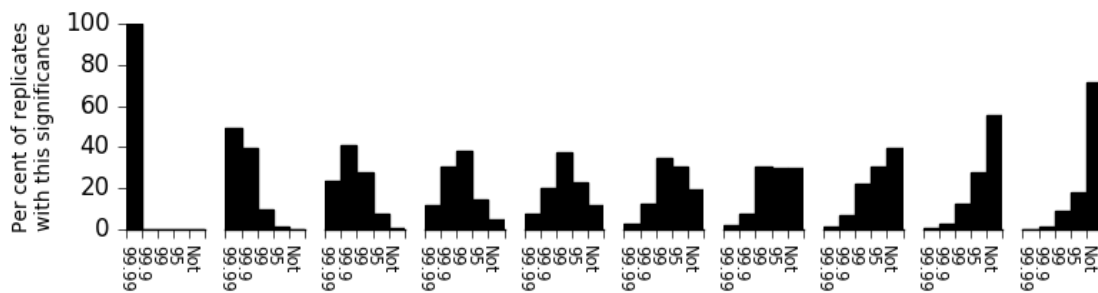
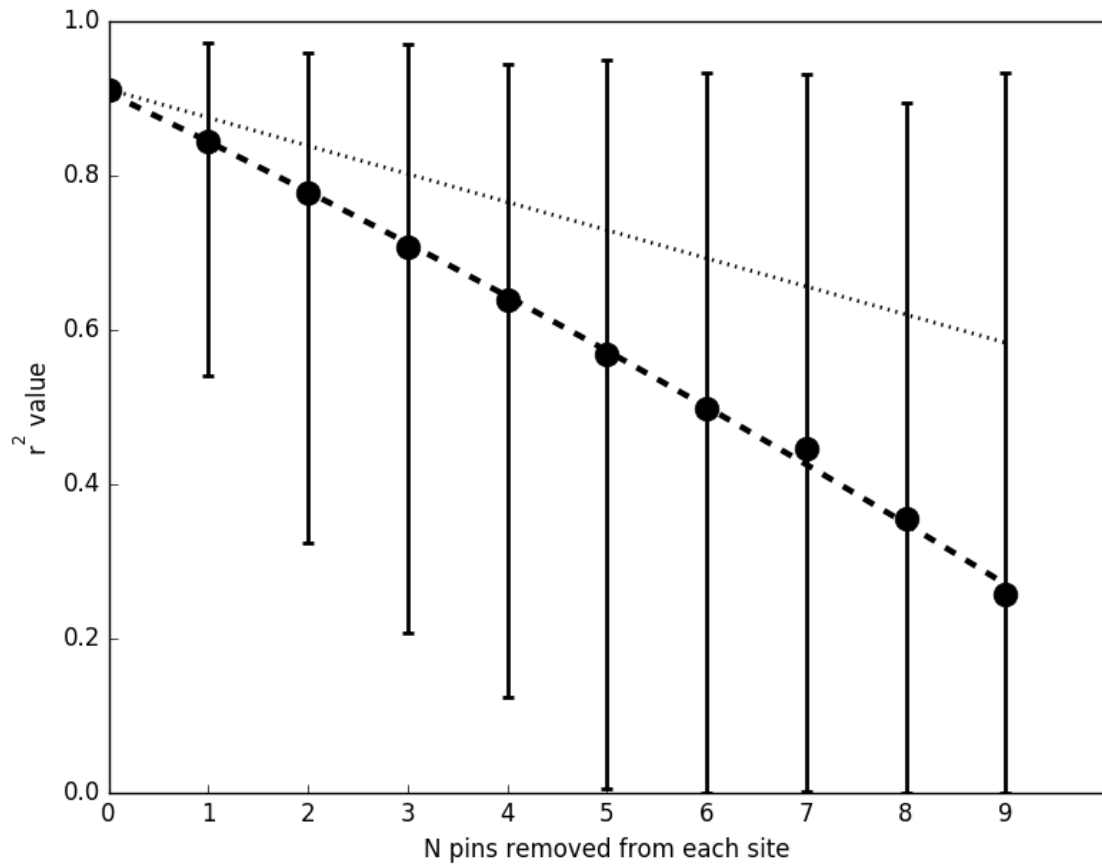


Figure 10. The regression shown in Figure 7 repeated with pins randomly omitted. Each black dots shows the mean of each set of 1000 replicates, the whiskers show the range. The small bar charts show the distribution of significance for each set of replicates. The dashed line is a best fit to the replicate means, the dotted line shows the 'naive assumption' where removal of one pin removes 1/25 of the predictive power, etc.